



## Pressure profile impact on batch reverse osmosis desalination: investigation and optimization

Abdeljalil Chougradi<sup>a,\*</sup>, Lalla Naima Qadiri<sup>b</sup>, Jamal-Eddine Jellal<sup>a</sup>

<sup>a</sup>Civil Engineering Department, Mohammadia School of Engineering, Mohammed V University in Rabat, Av. Ibn Sina B.P 765, Agdal Rabat 10090, Morocco, emails: chougradi.abdeljalil@gmail.com (A. Chougradi), jellaljamaledineemi@gmail.com (J.-E. Jellal)

<sup>b</sup>Department of Process Engineering, National School of Mineral Industries of Rabat, BP 753 Agdal, Rabat, Morocco, email: qadiri@enim.ac.ma

Received 20 April 2021; Accepted 17 August 2021

---

### ABSTRACT

Batch reverse osmosis (RO) is a recent emerging configuration for membrane desalination, which has the potential to reduce specific energy consumption (SEC) compared to continuous RO. In our study, we seek to explore the impact of different pressure profiles and process parameters on the batch RO behavior, and optimize the pressure profile to minimize SEC. The modeling and optimization were conducted based on our previously developed model implemented with differential evolution optimization code on Python. Three pressure different pressure profiles were considered to investigate batch RO behavior. For each pressure profile, the impact of feed salinity, feed volume, energy recovery device efficiency and pump efficiency on the batch RO energetic performance was examined. Results show that the process energetics and behavior depend directly on the applied pressure profile, which can be optimized for minimal energy use. Consequently, the batch RO under time-dependent flux also holds promising energy-saving potential. Interestingly, it was revealed that process parameters also affect the batch RO process energetics differently depending on the applied pressure profile.

*Keywords:* Batch desalination; Reverse osmosis; Water treatment

---

### 1. Introduction

Desalination has become a necessary alternative to provide clean water in the 21st century. This is because of global warming, irresponsible use of water, pollution and expanding economy. Desalination technologies have improved considerably in the last 50 years, and today, reverse osmosis membrane desalination is the most energy-efficient technology for desalination [1].

Reverse osmosis desalination operates, in most cases, in continuous configuration in one, two, or three stages. Depending on the recovery ratio, clean water is produced continuously and proportionally to feed flow rate. However, a new generation of discontinuous configurations called

batch and semi-batch, have emerged in the last decade [2–5]. The batch innovative configuration has been proved to reduce specific energy consumption [3,4] and to reach high recoveries with less potential of scaling [6] compared to continuous reverse osmosis (RO).

In the batch RO process (Fig. 1), feed water, which is stored in a tank, is pushed through the RO membrane by means of a pump. In our study, feed water flow rate is fixed while pump pressure it variable. The pump is adjusted to deliver the adequate pressure so that the net driving pressure (NDP) is constant in order to have a constant permeate flux or any desired NDP. Permeate is retrieved while brine is recirculated to feed storage. Pump pressure increases with time as feed osmotic pressure increases to

---

\* Corresponding author.

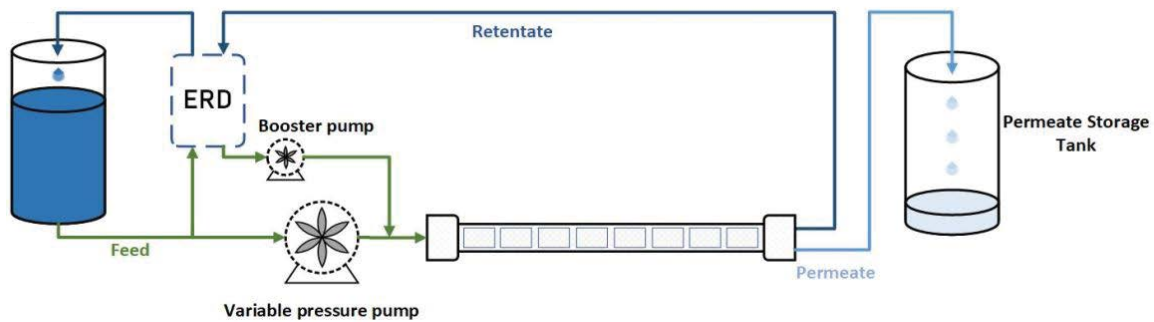


Fig. 1. Batch RO process scheme using energy recovery device to recover energy from recirculated brine. A variable pressure pump delivers time-dependent pressure, as feed osmotic pressure increases.

insure a positive permeate flux. An energy recovery device (ERD) is installed to recover energy from recirculated brine. The process continues until a stop condition is reached, such as feed osmotic pressure or pump pressure, which marks the end of a cycle. The feed tank is then emptied, refilled, and a new cycle starts again.

In our previous work [7], we have shown the energy-saving advantage of the batch RO configuration compared to the continuous RO configuration, as illustrated in Fig. 2. Salinities and fluxes were respectively 35 and 5 g/L, 15 LMH and 25 LMH for seawater and brackish water. The comparison showed that for seawater, batch RO can save energy for recovery ratios higher than 50% and that it's more energy efficient than continuous for all recovery ratios for brackish water. For seawater, it can save up to 31% energy for seawater at a recovery ratio of 60% and up to 34% for brackish water at a recovery ratio of 80%.

Different batch RO configuration models have been introduced in the literature [2,3,8,9], in order to describe the process and estimate its energetic performance compared to continuous RO configuration. They have highlighted that promising energy savings can be achieved for both seawater and brackish water, especially at high recoveries.

However, these works have only focused on batch RO operating under constant flux, that is, pump pressure was set so that the NDP is constant. None of the models considered a pressure profile that delivers a time variable flux. This idea was never explored to the best knowledge of the authors.

In this study, we used our previously introduced model [7], to investigate the batch RO configuration behavior under different pressure profiles with different time-dependent NDP. To that end, three different pressure profiles were introduced: one delivering constant flux and two producing time-dependent flux. The batch RO behavior, including specific energy consumption (SEC), concentration polarization and process time to reach a specific recovery ratio were investigated and shown to be unique to the applied pressure profile.

In order to explore the full energy-saving potential of the batch RO, optimization of pressure profile by differential evolution algorithm was considered. The purpose was to find the optimal pressure profile that could deliver the

lowest possible SEC for a specific recovery ratio. Moreover, the impact of process parameters on process behavior, such as initial feed salinity, initial volume, ERD efficiency and pump efficiency, were examined under different pressure profiles.

## 2. Methods

### 2.1. Reference to the batch RO model

The model used to study the batch process behavior [7] was previously established in our modeling paper of the batch RO. It was validated experimentally and by comparison with another model [9]. It allowed the estimation of the SEC as a function of the recovery ratio while taking into consideration key parameters: feed initial salinity, feed water volume in the storage tank, membrane surface, pump pressure profile, concentration polarization, ERD efficiency and pump efficiency. A python algorithm code was developed to solve the batch process differential equations. We reintroduce the batch process scheme in Fig. 3 and the major equations which describe the batch RO variables in Table 1.

### 2.2. Pressure profiles and case study parameters

The established model [7] allowed to monitor all the process variables and the SEC at all recovery ratios. The SEC equation is composed of three parts, which express in order: specific energy to produce permeate, specific energy to pressure brine and specific energy recuperated from pressurized brine. The model also allowed the application of different pressure profiles  $\Delta P(t)$ , whether to deliver constant NDP or time-dependent NDP. This feature allowed to explore the impact of pressure profiles on the batch RO behavior and its energetic performance. The parameters used for the behavior comparison are depicted in Table 1.

The following pressure profiles were considered:

- *Pressure profile 1*: pressure is constant (54 bar) during the entire process;
- *Pressure profile 2*: pressure is set so that the NDP is constant to produce 10 LMH;

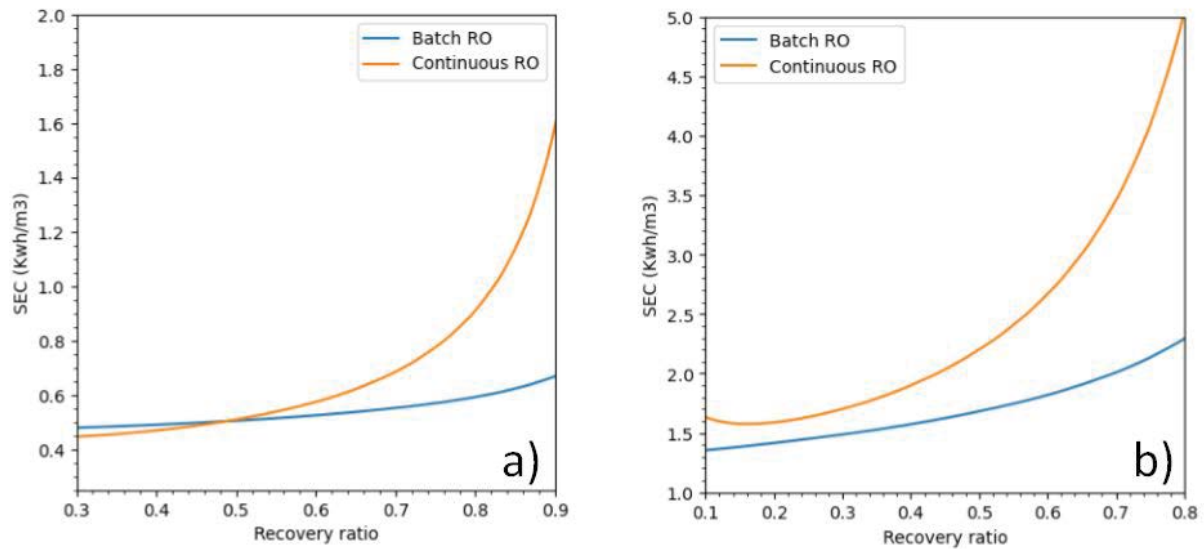


Fig. 2. SEC of batch RO and continuous RO vs. recovery ratio for seawater (a) and brackish water (b) [7].

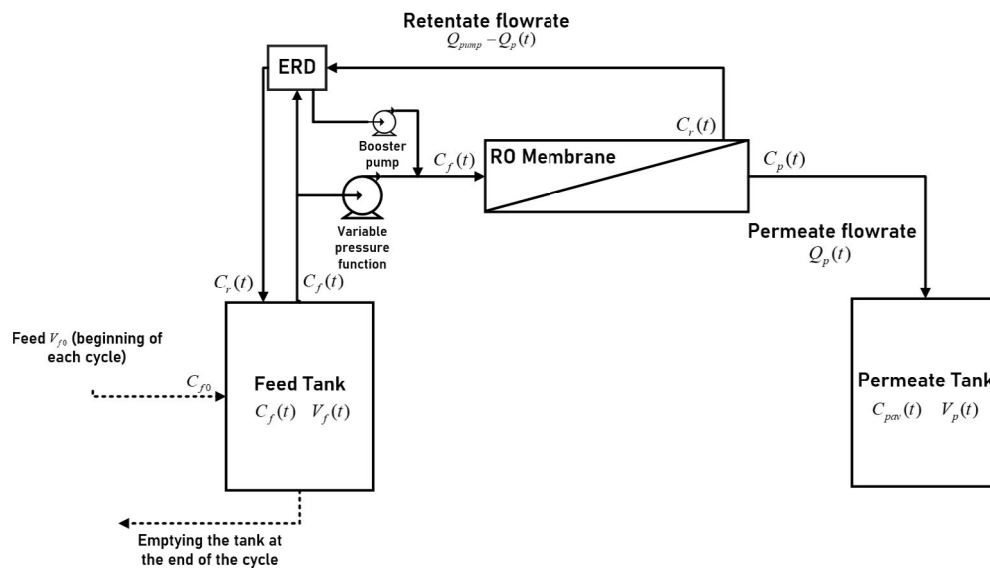


Fig. 3. Schematic diagram of the batch RO process [7].

- *Pressure profile 3*: pressure is a linear function: 32 bar + 35 bar/h;

2.3. Optimization strategy

After analyzing the impact of pressure profiles on the batch RO, differential evolution was adopted in order to find the optimal pressure profile to minimize SEC for a fixed recovery ratio. The differential evolution optimization method is widely used and approved in the optimization community [10]. It is based on natural selection and uses mutation and recombination to find the global optimal solution. The pressure profile was considered to have a polynomial form, the goal was then to find the

coefficients of the polynomial for the case study depicted in Table 2. Instead of looking for analytical expression using the nonlinear differential system equation, we considered a polynomial expression for the optimal pressure profile, as stated by the Weierstrass approximation.

3. Results and discussion

3.1. Effect of pressure profile on batch RO

The purpose of this part is to investigate the impact of pressure profile on the batch RO behavior under the three mentioned pressure profiles. To that end, we took interest in the following variables: pressure profiles with corresponding osmotic pressures, permeate fluxes, feed tank concentrations,

Table 1  
Batch RO model equations from [7] used in the present study

Computed variable or parameter	Equation
Osmotic pressure	$\Delta\pi_{CP}(t) = \Psi(C_m(t) - C_{p-CP}(t))$
Pressure delivered	$\Delta P(t) = \Delta P_{pump}(t) - \frac{\Delta L}{2}$
NDP	$NDP = \Delta P(t) - \Delta\pi_{CP}(t)$
Permeate concentration	$C_{p-CP}(t) = \frac{\sqrt{\left(\frac{A_w \Delta P(t)}{B_s} - \frac{A_w \Psi C_m(t)}{B_s} + 1\right)^2 + \frac{4A_w \Psi C_m(t)}{B_s}} - \left(\frac{A_w \Delta P(t)}{B_s} - \frac{A_w \Psi C_m(t)}{B_s} + 1\right)}{\frac{2A_w \Psi}{B_s}}$
Global system concentration equations	$\frac{dC_{pav-CP}(t)}{dt} = \frac{Q_{p-CP}(t)}{V_{p-CP}(t)}(C_{p-CP}(t) - C_{pav-CP}(t))$ $\frac{dC_{f-CP}(t)}{dt} = \frac{Q_{p-CP}(t)}{(V_{f0} - V_{p-CP}(t))}(C_{f-CP}(t) - C_{p-CP}(t))$
Concentration polarization (CP) equation	$\frac{C_m(t) - C_p(t)}{C_f(t) - C_p(t)} = \exp\left(\frac{J_v(t)}{k}\right)$
Permeate flowrate	$Q_{p-CP}(t) = J_{w-CP}(t) \cdot S$
Permeate volume	$V_{p-CP}(t) = \int_0^t Q_{p-CP}(x) dx$
Brine recirculated volume	$V_{r-CP}(t) = \int_0^t (Q - Q_{p-CP}(x)) dx$
Recovery ratio	$X_{CP}(t) = \frac{V_{p-CP}(t)}{V_{f0}}$
SEC	$SEC(t) = \frac{1}{\eta_{pump} V_{p-CP}(t)} \left[ \int_0^t \Delta P_{pump}(x) Q_{p-CP}(x) dx + \int_0^t \Delta P_{pump}(x) (Q - Q_{p-CP}(x)) dx - \eta_{ERD} \int_0^t \left( \Delta P_{pump}(x) - \frac{\Delta L}{2} \right) (Q - Q_{p-CP}(x)) dx \right]$

concentration polarization factors (CPF), recovery ratios and SECs (Fig. 4).

Pressure profiles 1 and 3 had a tendency to act as an asymptote for their corresponding osmotic pressures. Pressure profile 2 kept a constant difference with its osmotic pressure (Fig. 4a). Permeate flux varied proportionally to NDP for each case. It started at a high value of flux at the beginning of the process for pressure profile 1 then decreased considerably. For pressure profile 2, it was constant as intended. For the third case, it increased for the first 15 min of the process then decreased, according to the difference between pressure profile 3 and its corresponding osmotic pressure. (Fig. 4b).

Feed tank salt concentration increased rapidly for pressure profile 1 compared to pressure profiles 2 and 3 (Fig. 4c). This is due to the amount of permeate volume produced. The more permeate volume is higher, the more feed tank concentration increases, since salt will be trapped in the tank. Which explains why recovery ratios (Fig. 5e) and feed concentrations evolutions have similar trends.

Permeate tank concentration varied depending on pressure profile. In the first 30 min of process time, it was less than 500 mg/L for all pressure profiles (Fig. 4d), where the recovery ratio of all three cases was around 50%. Permeate tank concentration behavior depended on the feed concentration and the applied NDP for each case.

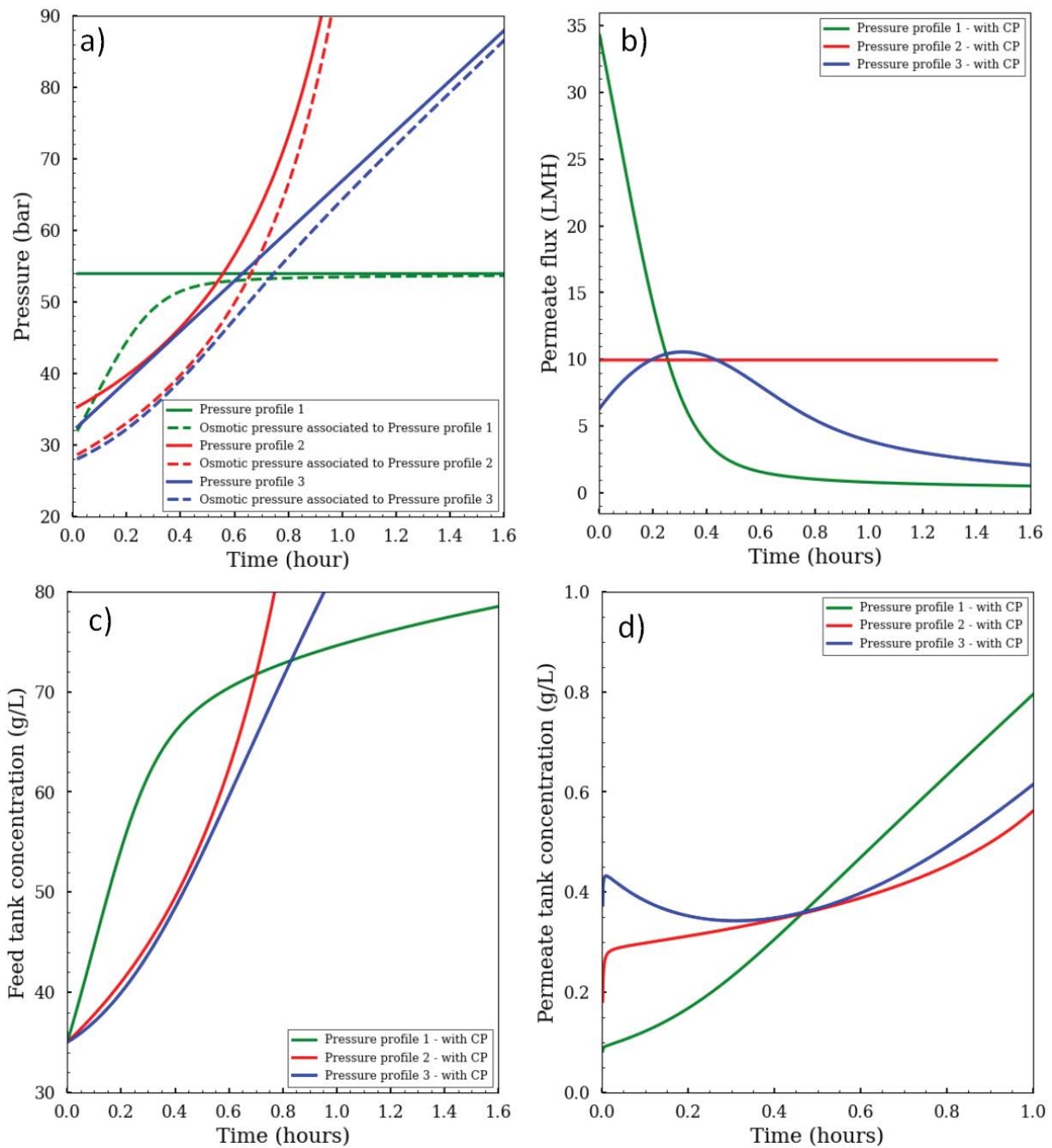


Fig. 4. Seawater batch RO process behavior is inspected under three different pressure profiles: 1, 2 and 3 against time, with or without CP. Salinity is 35 g/L, feed volume is 8 m<sup>3</sup>, and water permeability is 1.5 LMH/bar. (a) Pressure profiles and correspondent osmotic pressures, (b) permeate flux, (c) feed concentration, and (d) permeate tank concentration.

Recovery ratio behavior (Fig. 5e) is attributed to flux behavior. Since permeate production is constant for pressure profile 2, its corresponding recovery ratio is linear. Under constant pressure profile, recovery ratio increased rapidly before 25 min and then rose slowly, which is due to flux decreasing considerably after that moment.

CPF variation was also unique for each pressure profile (Fig. 5g). It exhibited similar behavior as flux permeate for all pressure profiles: the higher the NDP, the higher the

CPF. Concentration polarization (CP) affected recovery ratio as it caused it to slow down compared to when CP was not taken into consideration, for pressure profiles 1 and 3, as shown in Fig. 5e. CP didn't affect recovery ratio for pressure profile 2, because even if osmotic pressure increased due to CP, pump pressure was set to keep a constant NDP along the process. However, it did affect its SEC (Fig. 5f) compared to when CP was not taken into consideration because the delivered pump pressure was higher.

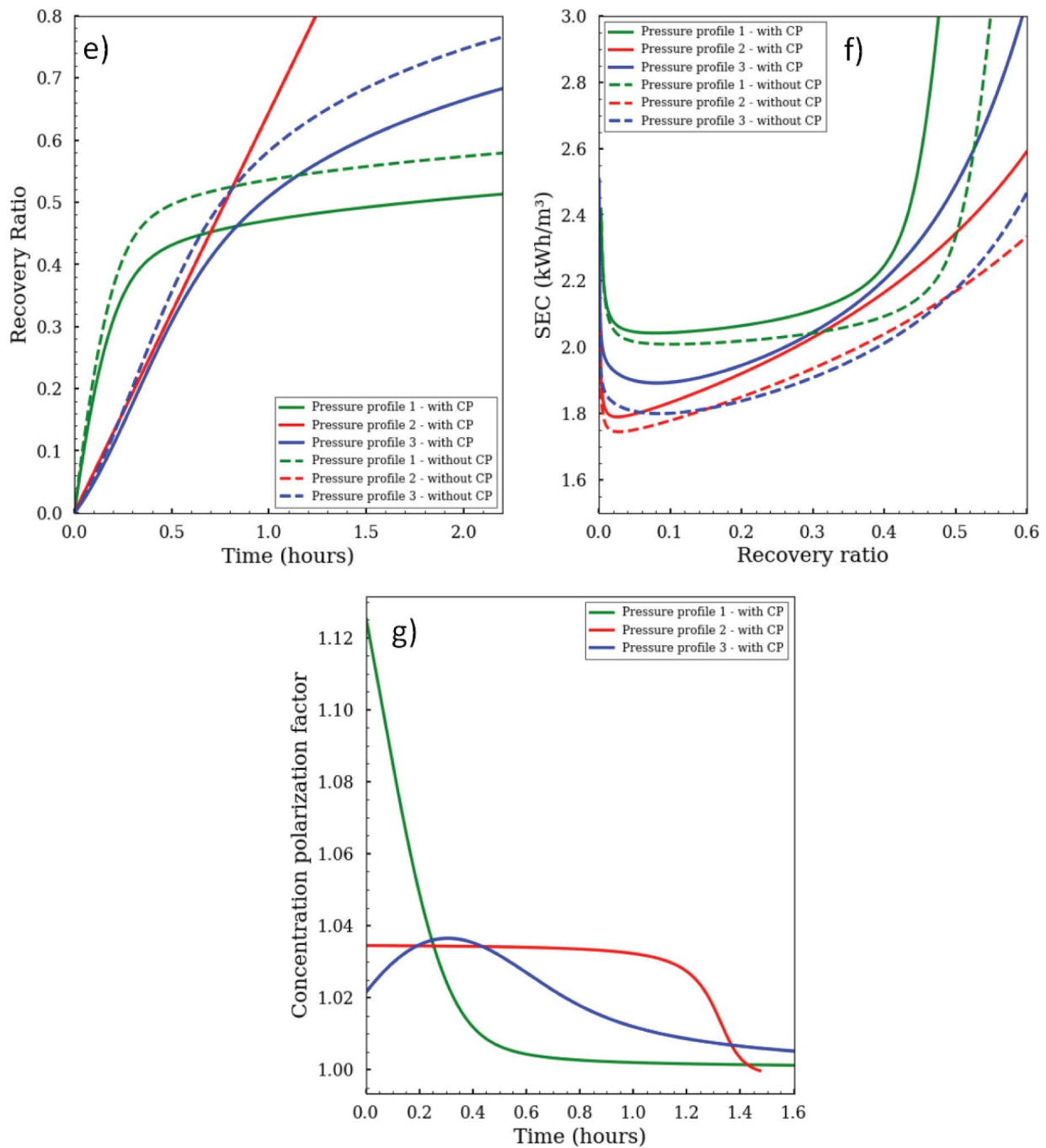


Fig. 5. Seawater batch RO process behavior is inspected under three different pressure profiles: 1, 2 and 3 against time, with or without CP. Salinity is 35 g/L, feed volume is 8 m<sup>3</sup>, and water permeability is 1.5 LMH/bar. (e) Recovery ratios with and without CP, (f) SEC with and without CP, against recovery ratio, and (g) CPF.

SEC depended directly on the applied pressure profile and CP. For all recovery ratios, pressure profile 1 had the highest SEC, followed by pressure profile 3 and pressure profile 2. When CP was not taken into account, pressure profile 1 had again the highest SEC while pressure profiles 2 and 3 had their rankings switched, because CP didn't have the same impact on the process energetics under the three pressure profiles.

The time required to achieve the same recovery ratio wasn't the same for all the pressure profiles neither. While it took less than half an hour for pressure profile 1 to reach 45%, it took over 1 h for pressure profiles 2 and 3. Reaching rapidly recovery ratio of 45% under pressure profile 1 was however at the price of a peak of CPF at the process beginning compared to pressure profiles 2 and 3 because NDP was higher at that moment.

### 3.2. Impact of pressure profile on salinity and feed volume variations

Initial feed salinity and feed volume have a high impact on the batch RO energetics. In this part, feed salinity and volume impact on batch RO SEC were investigated, under different pressure profiles.

Under pressure profile 2 (Fig. 6b), SECs for different salinities seemed to increase steadily with an average value of  $0.25 \text{ kWh/m}^3$  for every increase of  $5 \text{ g/L}$ . For pressure profiles 1 and 3 (Fig. 6a and c), this pattern was not sustained. The difference between SECs increased considerably at high recoveries under constant pressure, while it increased under linear pressure with no clear pattern.

Feed volume impact was also dependent on pressure profile. Under profile 2 (Fig. 7b), feed volume affected SEC

considerably when it was between  $0.25 \text{ m}^3$  and  $2 \text{ m}^3$  and only marginally beyond that. The feed volume impact seemed to manifest at recoveries below 30% and its effect was inverted at recoveries higher than 50%. Between 30% and 50%, SEC was interestingly independent of feed volume, where all cases delivered equal SECs. Under pressure profile 1 (Fig. 7a), the same behavior was observed, as between 30% and 45%, SEC was independent of the initial feed volume, however, the impact of feed volume was inverted outside this interval. The average SEC, however, decreased slowly before 45%, and then soared rapidly. While under pressure profile 2 it increased linearly after 10%. Under linear pressure profile (Fig. 7c), SEC evolution differed from the cases of pressure profiles 1 and 2. In fact, there was no intersection between the curves, and a clear correlation between feed volume increase and SEC decrease after 10% recovery was

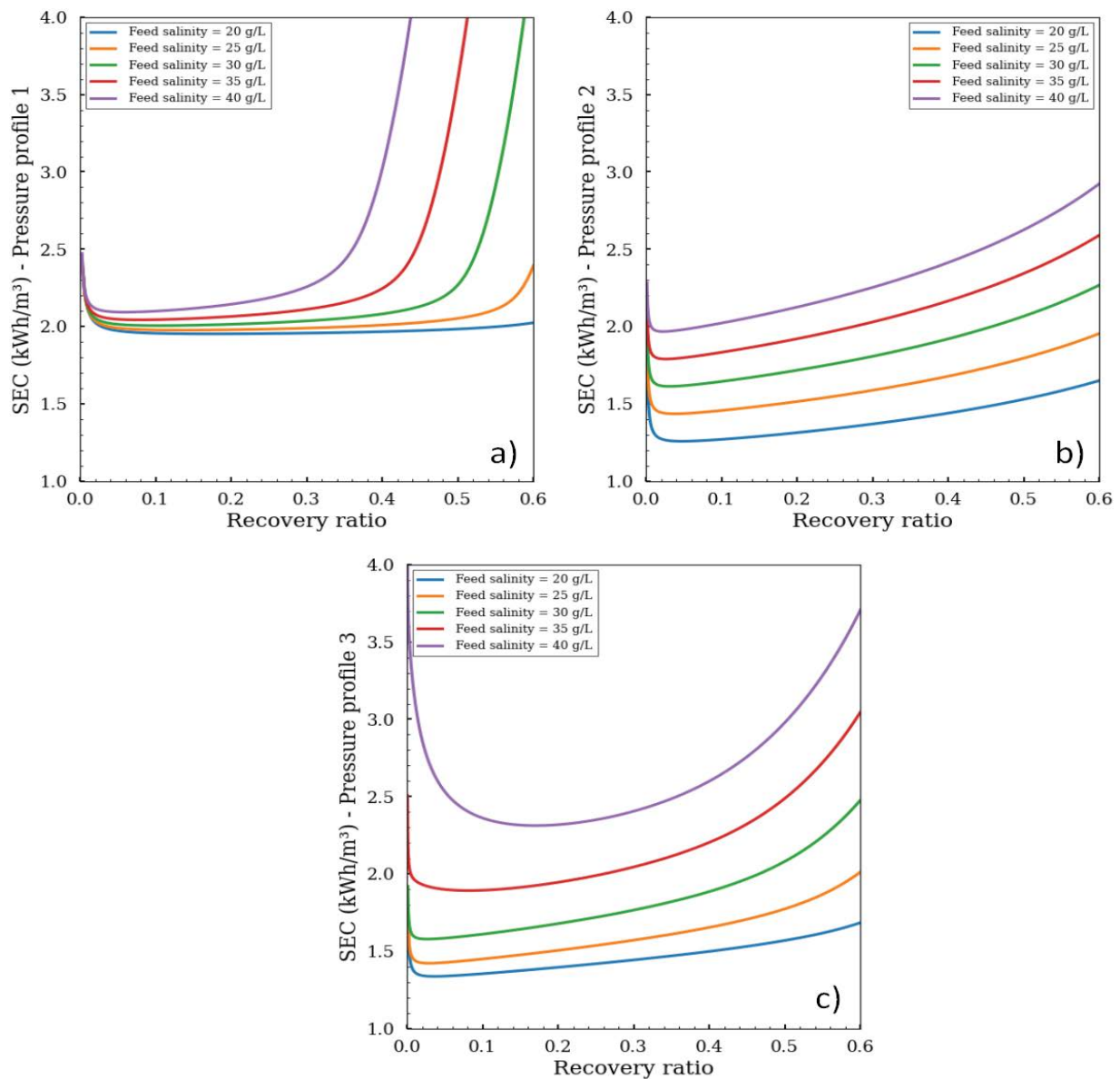


Fig. 6. Seawater batch RO energetic process behavior is inspected under various feed salinities, for pressure profiles 1 (a), 2 (b) and 3 (c) against recovery ratio, with CP taken into consideration. Feed volume is  $8 \text{ m}^3$ , and water permeability is  $1.5 \text{ LMH/bar}$ .

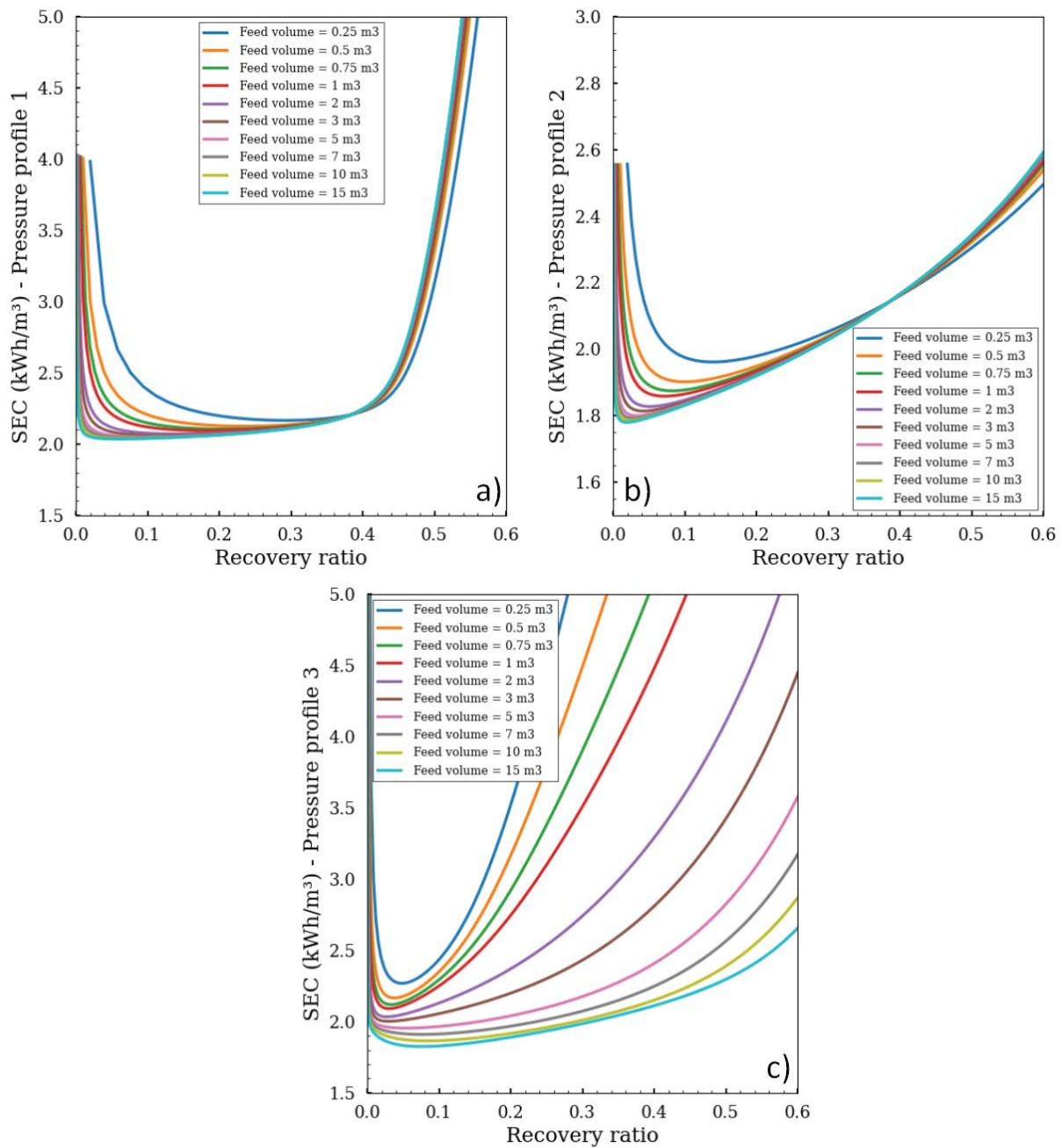


Fig. 7. Seawater batch RO energetic process behavior is inspected under various feed volumes, for pressure profiles 1 (a), 2 (b) and 3 (c) against recovery ratio, with CP taken into consideration. Salinity is 35 g/L, and water permeability is 1.5 LMH/bar.

observed. Moreover, SEC soared for lower feed volumes while it increased slowly for higher feed volumes.

Batch RO energetic behavior due to feed volume variation under different pressure profiles was partially unexpected. Under pressure profiles 1 and 2, the reason SEC varied considerably between 0.25 and 2 m<sup>3</sup> but varied less beyond that, is most probably caused by the dilution effect of brine recirculation. It is unclear, however, why there was an intersection zone where feed volume had no impact on energy use, and why there was an inversion of SEC plots outside that zone. Under pressure profile 3, feed volume

seemed to affect more directly the SEC of batch RO, where the lower the feed volume, the higher the SEC and the higher the slope.

Batch RO response under different salinities and different pressure profiles is mainly attributed to the unique permeate productions, given that the SEC is the ratio of spent energy to total permeate produced. Under pressure profile 2, even though salinity increased, pump pressure increased as well to keep constant flux, consequently, SEC increased steadily when feed salinity increased. However, under pressure profiles 1 and 3, increasing salinity meant increasing osmotic

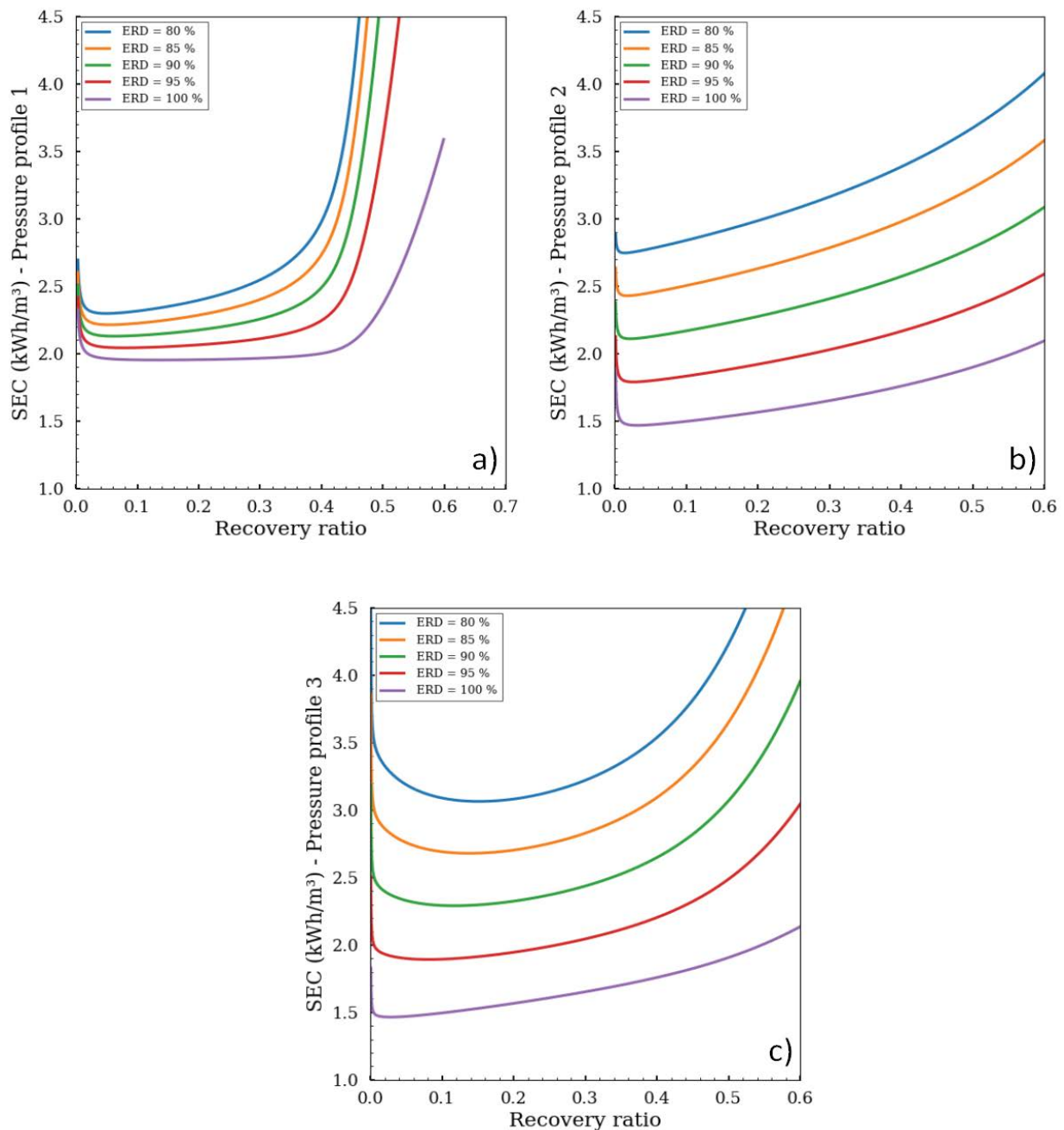


Fig. 8. Seawater batch RO energetic process behavior is inspected under various ERD efficiencies, for pressure profiles 1 (a), 2 (b) and 3 (c) against recovery ratio, with CP. Feed volume is  $8 \text{ m}^3$ , feed salinity is  $35 \text{ g/L}$  and water permeability is  $1.5 \text{ LMH/bar}$ .

pressure and thus reducing permeate flux, especially at the end of the process. This decrease in permeate flux explains energy use soaring the more the salinity increases and the higher the recovery ratio is.

### 3.3. Impact of pressure profile on ERD and pump efficiencies variations

ERD and pump efficiencies impacts on the batch RO energetics under various pressure profiles were investigated in this section. ERD affected directly the SEC

response, the higher its efficiency was, the less the SEC was. Under pressure 2 (Fig. 8b), SEC increased by about an average value of  $0.5 \text{ kWh/m}^3$  for every drop of 5% in efficiency. SEC plots seemed to follow the same allure and increased in parallel. Under pressure profile 3 (Fig. 8c), the same average increase of  $0.5 \text{ kWh/m}^3$  every 5% of efficiency was observed, however, the less the ERD efficiency, the more the energy tended to increase rapidly. Under pressure profile 1 (Fig. 8a), the same allure was sustained, with energy soaring after 40% for all ERDs, once permeate production decreased dramatically (Fig. 4b).

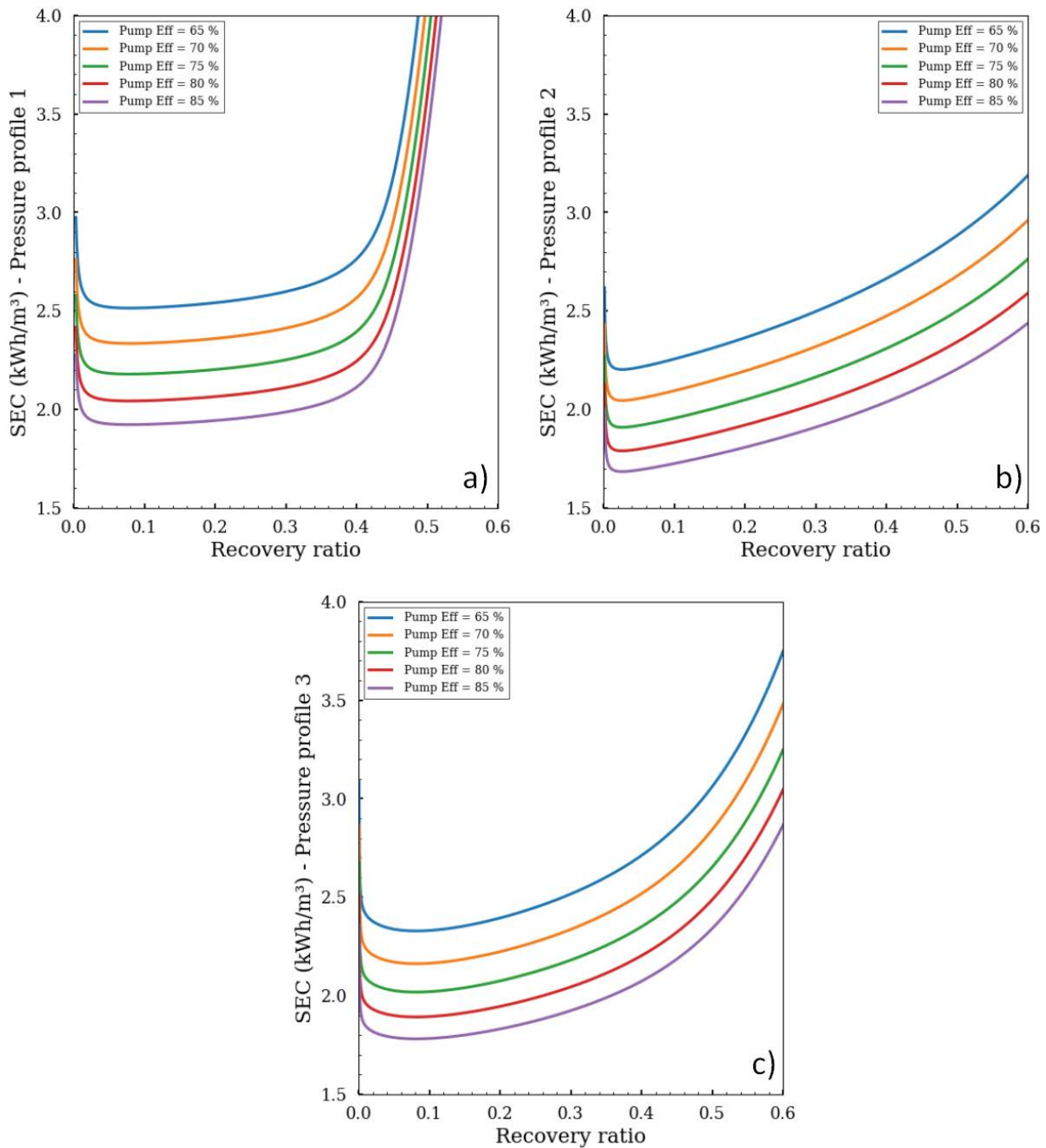


Fig. 9. Seawater batch RO energetic process behavior is inspected under various pump efficiencies, for pressure profiles 1 (a), 2 (b) and 3 (c) against recovery ratio, with CP. Feed volume is 8 m<sup>3</sup>, feed salinity is 35 g/L, and water permeability is 1.5 LMH/bar.

A common pattern among all three pressure profiles was observed: the loss in SEC, for every ERD efficiency drop by 5%, wasn't constant. It seemed to be around 0.5 kWh/m<sup>3</sup> on average and decreased when ERD efficiency declined.

Pump efficiency also affects directly the batch RO energetics under various pressure profiles. For all cases (Fig. 9), SEC trend of parallel curves was sustained. For the same 5% decrease in pump efficiency, under all pressure profiles, energy increased gradually.

The described behaviors, while they show pump efficiency impact on batch RO energetics, they can be explained mainly by the SEC expression in Table 2. When pump efficiency decreases, for a given pressure profile, the ratio (1/pump\_eff) increases, which explains why the SEC rises gradually when pump efficiency drops every 5%.

ERD efficiency impact under different pressure profiles is also attributed to the SEC expression. The term  $\eta_{ERD} \int_0^t (\Delta P_{pump}(x) - \Delta L)(Q - Q_p(x)) dx$  is the one responsible

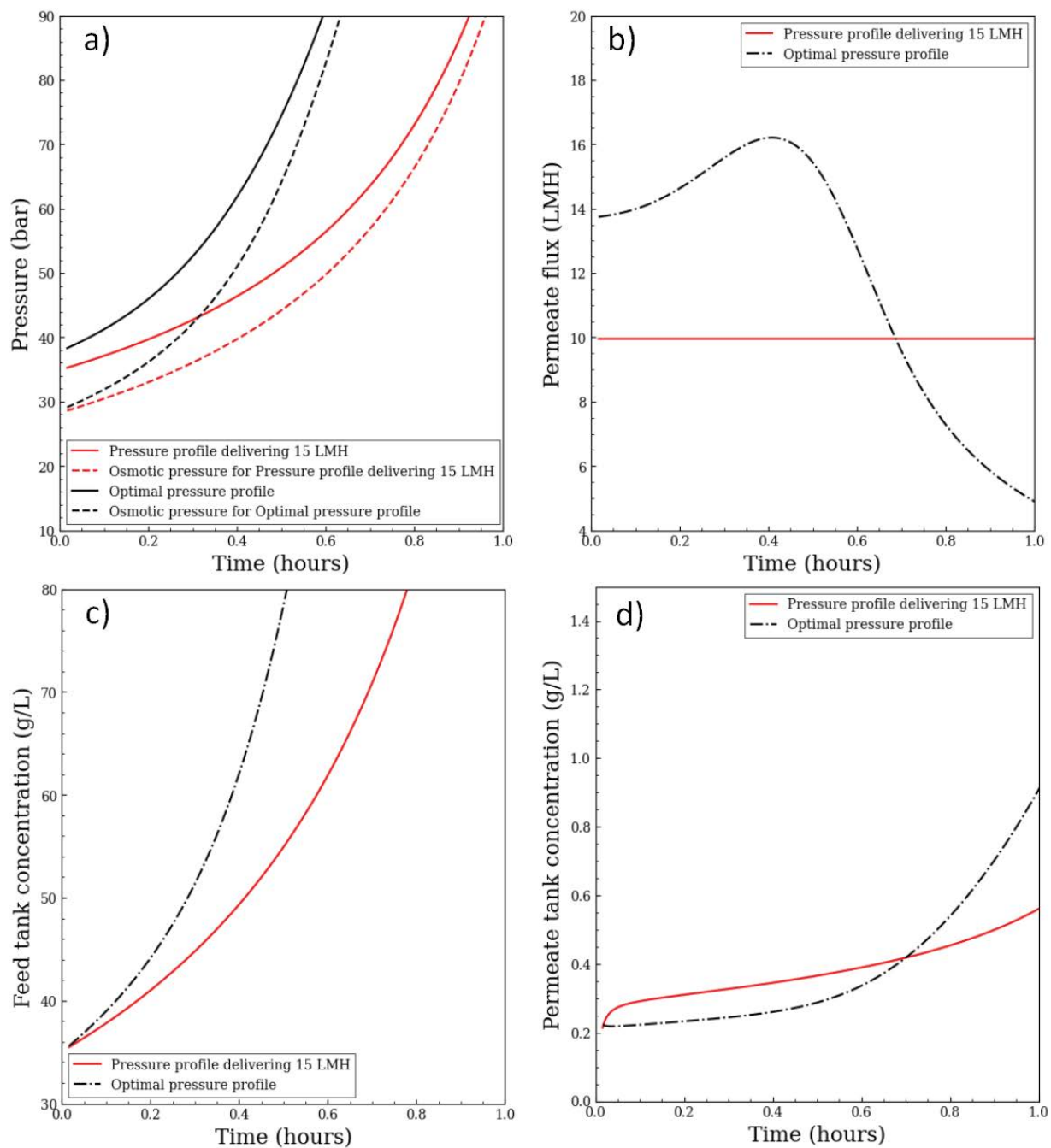


Fig. 10. Seawater batch RO process behavior is inspected under pressure profiles 1 and optimal pressure profile against time, with CP. Salinity is 35 g/L, feed volume is 8 m<sup>3</sup>, and water permeability is 1.5 LMH/bar. (a) Pressure profiles and correspondent osmotic pressures, (b) permeate flux, (c) feed tank concentration, and (d) permeate tank concentration.

for such behavior. The fact that each pressure profile is unique and produces a distinct flow rate is what causes the SEC patterns to be unique to each pressure profile.

#### 3.4. Optimal pressure profile to deliver minimal SEC at specific recovery rate

Following the previous sections, it was established that pressure profile impacts many aspects of the performance of

the batch RO process. In this section, the optimal pressure profile delivering the minimal SEC at a specific recovery ratio is investigated.

It should be noted that the pressure profile, which is the driving force behind the batch RO process, can be sorted into two types. The first type, like pressure profile 2, which depends on osmotic pressure, can deliver a permeate flux depending on the evolution of osmotic pressure. The second type of pressure profiles, like pressure profile 1 and 3, do not

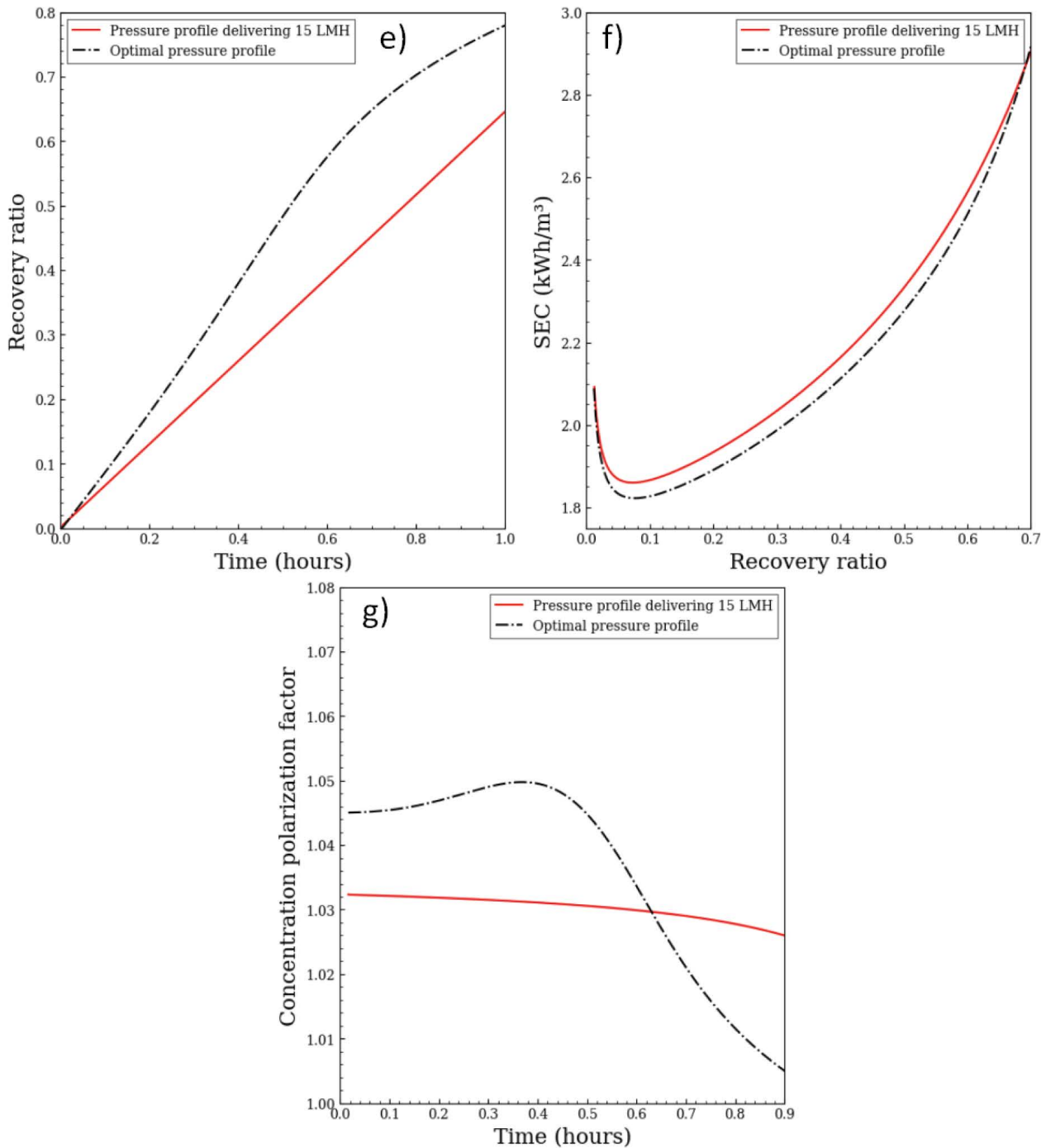


Fig. 11. Seawater batch RO process behavior is inspected under pressure profiles 1 and optimal pressure profile against time, with CP. Salinity is 35 g/L, feed volume is 8 m<sup>3</sup>, and water permeability is 1.5 LMH/bar. (e) Recovery ratios with and without CP, (f) SEC with and without CP against recovery ratio, and (g) CPF.

depend on osmotic pressure. Instead, it is the osmotic pressure that varies according to the profile pressure applied to the process.

The optimization of the first type of pressure profiles comprises reducing NDP to a minimum, approaching the thermodynamic limit, although NDP isn't necessarily constant in this case. However, it would take a long time to reach

the desired recovery ratio, and the pump working for a such duration could increase energy use. Moreover, it is not practical to have longer times to reach the desired recovery ratio. In our paper, we explore the optimization of the second type of pressure profiles.

To that end, optimal pressure profile was considered as a polynomial, which coefficients were subject to optimization.

Table 2  
Parameters used to compare the impact of pressure profiles on batch RO for seawater

Parameter	Value
Intake feed salinity for seawater, g NaCl/kg	35
Membrane element area, m <sup>2</sup>	37
Total elements in system (1 element per pressure vessel)	14
Membrane water permeability, LMH/bar	1.5
High-pressure pump efficiency	0.8
ERD efficiency	0.95
Total pressure drop, bar	1
Salt permeability, m/s	$2.21 \times 10^{-8}$
Feed tank volume, m <sup>3</sup>	8
Mass transfer coefficient, m/s	$8 \times 10^{-5}$
Feed flow (constant), m <sup>3</sup> /h	32.4

Differential evolution optimization algorithm in Python was conducted, to find the global minimum of energy use SEC at recovery ratio 45%. The choice of polynomial order was taken according to energy savings performance and computer processing speed. We considered the fourth-order, because using the fifth-order polynomial improved negligibly the energy savings and caused the computing machine to take non-practical time to run the algorithm.

We used the differential evolution algorithm because it allows to find the global minimum of a multimodal search independently of initial parameters values while converging rapidly with few control parameters. This algorithm is adapted for numeric optimization problems given that it is a population-based algorithm like genetic algorithm using operations like crossover, mutation and selection.

The optimization algorithm for the case in the previous section delivered the following optimal pressure profile:

$$\Delta P_{\text{optimal}}(t) = 3,787,951.04 + 839.72t + 0.267803t^2 + 2,030,183 \times 10^{-4}t^3 + 1.2344 \times 10^{-8}t^4 \quad (1)$$

$$[a_0, a_1, a_2, a_3] = [(0, 6000000), (0, 100000), (0, 1000), (0, 1000), (0, 1000)]$$

where pressure is in Pa and time in s.

The optimal pressure profile was simulated on the Batch RO process using the same parameters as in the previous section, and was compared to pressure profile 2. SEC comparison between the three pressure profiles (Fig. 5f) showed that pressure profile 2 delivered the best energetic performance at a recovery ratio of 45%. Performance comparison of batch RO under pressure profile 2 and optimal pressure is shown in Figs. 10 and 11.

Indeed, the SEC of batch RO under the optimal pressure was lower at recovery 45% (2.19 kWh/ m<sup>3</sup> compared to 2.24 kWh/ m<sup>3</sup> delivered by profile 2 (Fig. 11f), and at all recovery ratios. The process under optimal pressure profile also took less time to reach a recovery ratio of 45% as shown in Fig. 11e. The NDP for optimal pressure and permeate flux (Fig. 10b) were respectively time-dependent

and constant, consequently, the CPF had similar allure (Fig. 11g). Osmotic pressure (Fig. 10a) and feed concentration (Fig. 10c) increased quickly under optimal pressure profile compared to pressure profile 2, because permeate production was higher due to higher permeate flux at the beginning of the process.

Optimization allowed to reduce SEC and gain in process time. Using an optimal pressure profile can draw the full potential of the batch RO process. Although the energetic gain wasn't significant, it proved that optimizing the pressure profile can allow to further reduce energy use of Batch RO.

#### 4. Conclusion

Batch RO process behavior was investigated under different pressure profiles and optimal pressure profile. Findings of this study showed that pressure profiles can affect considerably the process behavior, including energetics, time to reach recovery ratio and concentration polarization. Each pressure profile had its unique impact. Constant pressure profile allowed reaching recovery ratio 45% rapidly but at the cost of SEC and high CP at the beginning of the process. Pressure profiles delivering constant flux and linear pressure delivered lower SEC with less risk of peak CPF, but took more time to achieve a recovery ratio of 45%.

Interestingly, the impact of process parameters was different under different pressure profiles. Varying feed salinity, feed volume, pump and ERD efficiencies affected SEC differently for each case depending on recovery ratio. The most remarkable impact was that of the feed volume, where under constant and parallel pressure, there were intervals of recovery ratio where feed volume didn't affect the SEC. This feature can be useful in the design of the feed tank volume for the batch RO process.

Optimization provided evidence that batch RO energy saving potential can be maximized. In fact, under optimal pressure profile, batch process used less SEC at 45% recovery compared to other pressure profiles and had its process time reduced.

Batch RO technology is still at the beginning of the development and research stage, further investigation on its different aspects is still needed to master its process and draw its full potential as a future alternative to classic continuous reverse osmosis.

#### Symbols

$A_w$	—	Solvent permeability constant, m <sup>2</sup> s/kg
$B_s$	—	Solute permeability constant, m/s
$C$	—	Concentration, kg/m <sup>3</sup>
$J_s$	—	Solute flux, kg/m <sup>2</sup> s
$J_w$	—	Solvent flux, m <sup>3</sup> /m <sup>2</sup> s
$k$	—	Mass transfer coefficient, m/s
$\Delta P$	—	Applied pressure, Kg/s <sup>2</sup> m
$\Delta P_{\text{pump}}$	—	Pump applied pressure, Kg/s <sup>2</sup> m
$Q$	—	Flowrate, m <sup>3</sup> /s
$S$	—	Membrane surface area, m <sup>2</sup>
$t$	—	Time, s
$V$	—	Volume, m <sup>3</sup>

$X$	—	Batch recovery ratio
$Q$	—	Flow rate $\text{m}^3/\text{s}$
$\pi$	—	Osmotic pressure, $\text{Kg}/\text{s}^2\text{m}$
$\psi$	—	Osmotic pressure to solute concentration ratio, $\text{m}^2/\text{s}^2$
$\Delta L$	—	Head loss, $\text{Kg}/\text{s}^2\text{m}$
$\eta_{\text{pump}}$	—	Pump efficiency
$\eta_{\text{ERD}}$	—	ERD efficiency
LMH	—	permeate flux unit, $\text{L}/\text{m}^2/\text{h}$

### Subscripts

$f$	—	Feed tank
$f_0$	—	Feed tank at time = 0
$p$	—	Permeate at membrane outlet
pav	—	permeate in the tank
$r$	—	Recycled brine
$m$	—	Membrane wall
CP	—	Means CP is taken into account in computing

### References

- [1] M. Elimelech, W.A. Phillip, The future of seawater desalination: energy, technology, and the environment, *Science*, 333 (2011) 712–717.
- [2] J.R. Werber, A. Deshmukh, M. Elimelech, Can batch or semi-batch processes save energy in reverse-osmosis desalination?, *Desalination*, 402 (2017) 109–122.
- [3] D.M. Warsinger, E.W. Tow, K.G. Nayar, L.A. Maswadeh, J.H. Lienhard V, Energy efficiency of batch and semi-batch (CCRO) reverse osmosis desalination, *Water Res.*, 106 (2016) 272–282.
- [4] A. Efraty, R.N. Barak, Z. Gal, Closed circuit desalination — a new low energy high recovery technology without energy recovery, *Desal. Water Treat.*, 31 (2011) 95–101.
- [5] A. Efraty, R.N. Barak, Z. Gal, Closed circuit desalination series no-2: new affordable technology for sea water desalination of low energy and high flux using short modules without need of energy recovery, *Desal. Water Treat.*, 9 (2012) 189–196.
- [6] D.M. Warsinger, E.W. Tow, L.A. Maswadeh, G.B. Connors, J. Swaminathan, J.H. Lienhard V, Inorganic fouling mitigation by salinity cycling in batch reverse osmosis, *Water Res.*, 137 (2018) 384–394.
- [7] A. Chougradi, F. Zaviska, A. Abed, J. Harmand, J.-E. Jellal, M. Heran, Batch reverse osmosis desalination modeling under a time-dependent pressure profile, *Membranes*, 11 (2021) 173, doi: 10.3390/membranes11030173.
- [8] J. Swaminathan, E.W. Tow, R.L. Stover, J.H. Lienhard V, Practical aspects of batch RO design for energy-efficient seawater desalination, *Desalination*, 470 (2019) 114097, doi: 10.1016/j.desal.2019.114097.
- [9] Q.J. Wei, C.I. Tucker, P.J. Wu, A.M. Trueworthy, E.W. Tow, J.H. Lienhard V, Impact of salt retention on true batch reverse osmosis energy consumption: experiments and model validation, *Desalination*, 479 (2020) 114177, doi: 10.1016/j.desal.2019.114177.
- [10] R. Storn, K. Price, Differential evolution – a simple and efficient heuristic for global optimization over continuous spaces, *J. Global Optim.*, 11 (1997) 341–359.